Biogas sparging to control fouling and enhance resource recovery from anaerobically digested sludge centrate by forward osmosis

Revised version submitted to

Journal of Membrane Science

December 2020

Minh T. Vu[a], Luong N. Nguyen[a], Md Abu Hasan Johir[a], Xiwang Zhang[b], Long D. Nghiem[a, c*], and Menachem Elimelech[d],

[a] Centre for Technology in Water and Wastewater, School of Civil and Environmental Engineering, University of Technology Sydney, NSW 2220, Australia

[b] Department of Chemical Engineering, Monash University, Room 213, Building 36, 18 Alliance Lane, Clayton Campus, Clayton Vic, 3800, Australia

[c] NTT Institute of Hi-Technology, Nguyen Tat Thanh University, Ho Chi Minh City, Vietnam

[d] Department of Chemical and Environmental Engineering, Yale University, New Haven, CT 06520-8286, United States

*Corresponding author

Long D. Nghiem, Centre for Technology in Water and Wastewater, School of Civil and Environmental Engineering, University of Technology Sydney, NSW 2007, Australia (E-mail: DucLong.Nghiem@uts.edu.au)

Graphical abstract

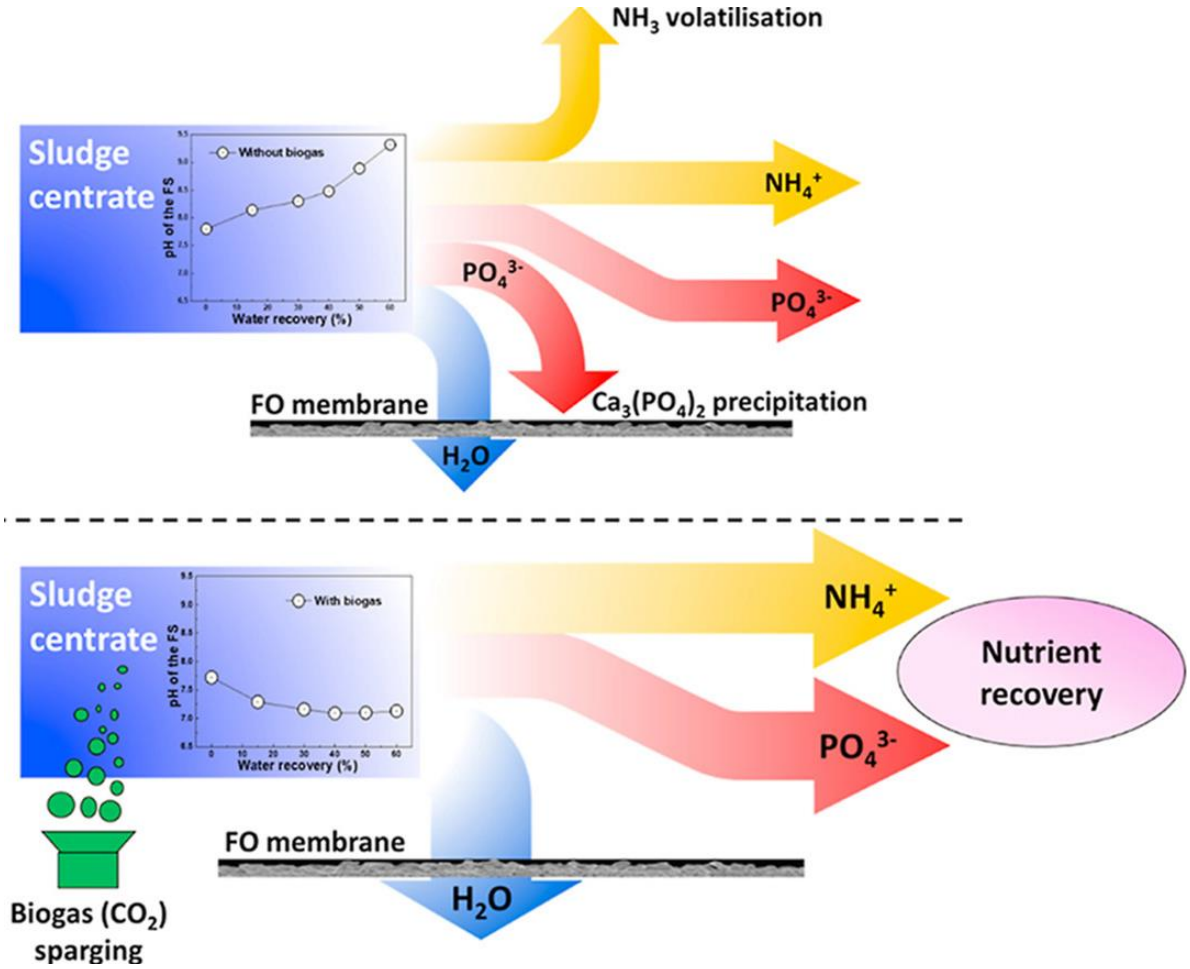

Highlights

- Proof-of-concept to biogas sparging to improve carbon and nutrient enrichment by FO.
- Biogas sparging reduced membrane fouling and enhanced nutrient recovery.
- Membrane fouling was fully reversible by physical flushing.
- Near neutral pH was maintained to prevent PO_4^{3-} precipitation & NH_3 volatilization.

Abstract

This study demonstrates the proof-of-concept of biogas sparging to control membrane fouling during sludge centrate pre-concentration by forward osmosis (FO). Sludge centrate sparging by biogas reduced membrane fouling (measured by flux decline) and filtration time by two and eight times, respectively compared to FO operation without biogas sparging at the same water recovery of 60%. In addition, the water flux was almost fully recovered by physical flushing when biogas sparging was applied. Biogas sparging also resulted in a significant improvement in the enrichment of organic, ammonia, and phosphate to close to the theoretical value based on mass balance calculation. In other words, organic matter and nutrients were retained in the bulk solution for subsequent recovery. Fouling mitigation and nutrient enrichment improvement by biogas sparging could be attributed to carbonate buffering to maintain a near neutral pH for preventing calcium phosphate precipitation on the membrane surface and ammonia volatilisation.

Keywords: Forward osmosis; Anaerobic co-digestion; Membrane fouling; Biogas sparging; Nutrient recovery.

1. Introduction

Anaerobic digestion is extensively applied to treat organic wastes such as sewage sludge, food waste, and crop residue and produce energy in the form of biogas [1, 2]. In addition to biogas, anaerobic digestion also generate a liquid stream known as sludge centrate and a solid product commonly called biosolids [3]. The sludge centrate is rich in nutrients (i.e. ammonia and phosphate), thus, must be returned to the head of work for treatment or treated separately [4].

Sludge centrate from anaerobic digestion is both a problem and an opportunity. Returning sludge centrate to the head of work results in the accumulation of nutrients, possible nutrient overloading and potential struvite blockage [5]. Uncontrolled nutrient release to the aquatic environment can cause eutrophication and even harmful algae blooms [6]. On the other hand, the high ammonia and phosphate content in sludge centrate makes it an ideal target for nutrient recovery for fertilizer production and other industrial applications [7-9].

Phosphorus can be directly extracted from sludge centrate as struvite, calcium phosphate, or vivianite by chemical precipitation using commercially available processes such as Phosnix, Ostara, and P-RoC. The efficiency of these commercial processes depends on initial phosphorus level. Low level of phosphorus requires more chemical addition and longer crystal retention time, thus higher operational costs. To increase the economics of nutrient recovery, sludge centrate is pre-concentrated prior to chemical precipitation [10]. Forward osmosis (FO) has been identified as an ideal platform for enriching nitrogen and phosphorus in sludge centrate [10-12]. Low fouling propensity, high fouling reversibility, and low energy consumption especially when seawater can be used as the draw solution have made FO an ideal technology for pre-concentrating complex and challenging feed solutions without any pre-treatment [11, 13-18]. Numerous FO studies have been recently reported to explore the enrichment of nutrients in sludge centrate for subsequent recovery [4, 5, 19-21].

Previous studies have demonstrated the feasibility of using a seawater-driven FO system to pre-concentrate nutrients and organic matter in sludge centrate for subsequent resource recovery [5, 20]. Seawater is freely available in coastal areas and the spent draw solution can be returned directly to the ocean without further treatment. These studies also highlighted the challenge to control fouling due to the deposition of the phosphate precipitates directly on the membrane surface during the enrichment process. Vu et al. (2019) proposed to buffer the seawater draw solution using acetate to control the increase of sludge centrate pH during the filtration, thus hindering nutrient precipitation [5]. Although they have successfully

demonstrated this technique with experimental data, using acetate to buffer seawater is unlikely to be economically practical.

CO_2 from biogas can provide acidity to the sludge centrate to maintain low pH for fouling mitigation. It is hypothesized that phosphate precipitation and ammonia volatilisation can be prevented by the addition of CO_2 to the sludge centrate prior to the FO process. In other words, the equilibrium of CO_2 in biogas in aqueous solution can act as a buffer system to maintain low pH of sludge centrate, thereby preventing the formation of phosphate precipitates and ammonia volatilisation.

In this work, the effectiveness of using biogas pH buffering in terms of fouling mitigation, organic matter and nutrient enrichment is examined. Major mechanisms governing the biogas buffering of sludge centrate are elucidated and discussed. Results from this study contribute to the current effort to recover nutrients from wastewater and organic waste. Use of biogas produced in place from anaerobic digestion of sewage sludge to facilitate the resource recovery from sludge centrate which is also a by-product of this process would be a very sustainable and economical approach due to no requirements of chemical addition and transportation.

2. Materials and methods

2.1. Materials

Flat-sheet commercial thin film composite polyamide (TFC PA) membrane was obtained from Porifera, Inc. (Hayward, California, USA). Membrane samples were soaked into deionized (DI) water over night for complete hydration before use. The physiochemical properties of the membrane (i.e. water permeability (A), solute permeability (B), structural parameter (S), NaCl and Ca rejections) were characterized using nanofiltration and FO protocols reported elsewhere [22].

Seawater collected from Bondi Beach, Sydney, NSW, Australia was used as a draw solution (DS). The obtained seawater was pretreated using 0.45 μm filter paper before use. The filtered seawater has pH of 8.06 ± 0.03 and total dissolved salt of 30 g/L. The concentrations of Ca^{2+} and Mg^{2+} in this seawater were 440 and 1270 mg/L, respectively.

Digested sludge centrate denoted as sludge centrate was obtained from a high speed centrifuge of a WWTP in Sydney and used as a feed solution (FS). Key properties of this sludge centrate are summarized in Table 1.

Table 1. Characteristics of sludge centrate (values indicated average ± standard deviation of at least three samples).

Parameters	Unit	Sludge centrate
pH	-	7.75 ± 0.04
Electrical conductivity	mS/cm	12.74 ± 0.68
Total solids	g/L	1.2 ± 0.2
COD	mg/L	440 ± 14
Phosphate (PO_4^{3-})	mg/L	421 ± 17
Ammonia (NH_3-N)	mg/L	1141 ± 21
Total N (TN)	mg/L	1368 ± 11
Calcium (Ca^{2+})	mg/L	49.0 ± 3.1
Magnesium (Mg^{2+})	mg/L	5.8 ± 0.3

2.2. Anaerobic co-digestion and forward osmosis system

2.2.1. Forward osmosis with biogas sparging

The FO system (Figure 1) consisted of an acrylic glass cross-flow membrane cell, two variable speed gear pumps (Micropump, Vancouver, Washington, USA), conductivity meters, and a digital balance to measure the flux. The feed and draw solutions were circulated through the two symmetric rectangular semi-cells of the FO membrane module at the same cross-flow velocity of 12 cm/s in a counter-current mode. The internal dimensions of each semi-cell were 10 cm in length, 2 cm in width and 0.2 cm in height. In other words, the effective membrane area was 20 cm^2. The FO membranes were orientated either in active layer facing the FS (FO mode), or active layer facing the DS (PRO mode).

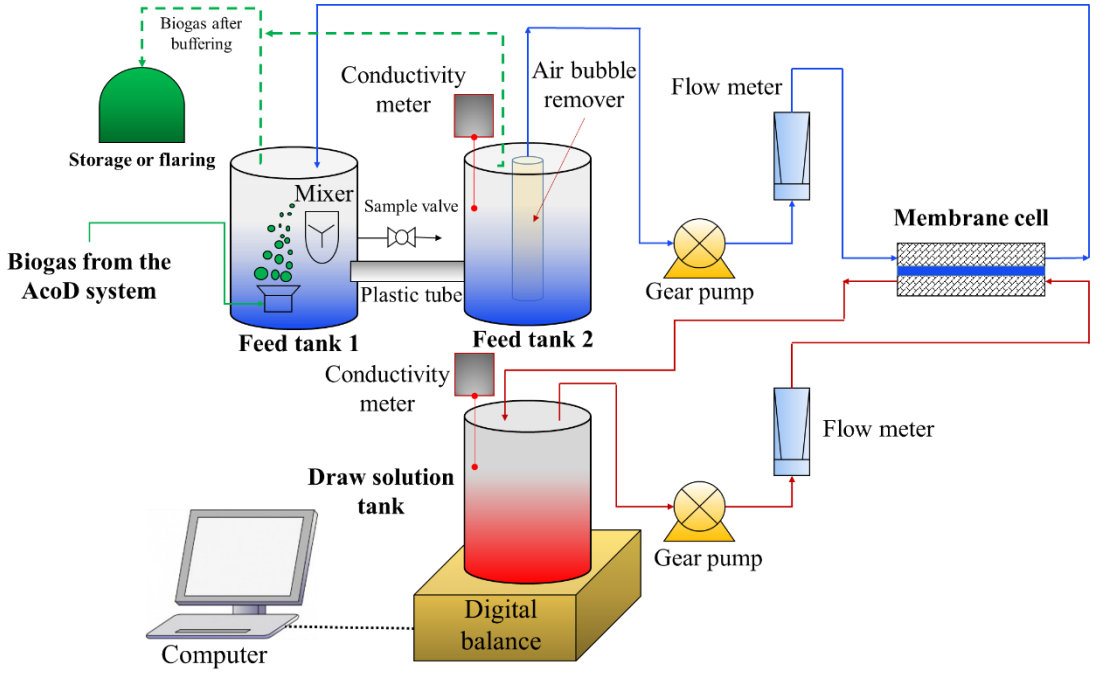

Figure 1. Schematic diagram of an anaerobic co-digestion and forward osmosis system for organic carbon and nutrient enrichment for subsequent resource recovery.

Two cylindrical plastic containers connected via a plastic tube were used to provide FS to the FO membrane cell (Figure 1). In the first feed container (i.e. feed tank 1), agitation and biogas sparging were carried out. The FS was then transferred to the second container where precipitate settling took place to minimize the impacts of agitation on membrane fouling as reported in a previous study [5]. Moreover, this design also reduced the transfer of biogas bubbles to FO membrane cell unit. Biogas from anaerobic co-digestion system was introduced via an air-stone diffuser at the bottom of the feed tank 1. After the buffering process, the remaining biogas is stored in a plastic gas bag for disposal by flaring. The retentate from the membrane cell was returned to the feed tank 1. In the second feed container (i.e. feed tank 2), an air-bubble remover was inserted inside to minimize the interference of air bubbles to the FO system (Figure 1). This bubble remover is a composite mesh with small pores (i.e. pore diameter of approximately 150 μm) in tubular configuration, which allows the passage of liquid, but not air bubbles. The feed solution moving into the membrane cell was withdrawn from the inside of this bubble remover.

2.2.2. Biogas

Biogas was obtained from a small-scale anaerobic digestion (AD) system (Figure S1). The system included a 28 L stainless steel conical reactor, two peristaltic hose pumps (DULCO® Flex from Prominent Fluid Controls, Australia) and a biogas counter (RITTER, MilliGascounter, Germany). A water bath (Thermo Fisher Scientific, Australia) was utilized to

maintain the temperature of the anaerobic reactor at 35 ± 0.5 °C by circulating hot water from the water bath through a rubber tube that was firmly wrapped around the reactor. Polystyrene foam and aluminium foil were employed to insulate the reactor.

Raw sewage sludge for anaerobic co-digestion operation was collected from a WWTP in Sydney, Australia. The digested sludge centrate used for seeding the anaerobic digester was also taken from the same WWTP. After arrival, sewage sludge and beverage waste were stored at - 4 °C in the dark and used within 2 weeks. Beverage waste was obtained a commercial waste collector and used as a co-substrate to ensure a continuous supply of biogas to the FO experiment. This beverage waste is a mixture of soft drinks unsuitable for consumption (e.g. out of date, contamination and damaged packaging). Key properties of the beverage waste and sewage sludge are presented in Table 2.

Table 2. Sewage sludge and beverage waste characteristics (values indicated average ± standard deviation of at least three samples)

Feed stock	COD (g/L)	pH	Total solid (%)	Volatile solid (%)
Sewage sludge	31.7 ± 2.5	5.46 ± 0.29	1.95 ± 0.20	1.76 ± 0.17
Beverage waste	125.8 ± 1.3	4.84 ± 1.12	0.04 ± 0.00	0.04 ± 0.00

The anaerobic digester was inoculated with 15 L of digested sludge from a WWTP in Sydney. Every day, 750 mL of digestate was withdrawn and replaced with the same volume of feed to maintain sludge retention time of 20 days. The anaerobic digester was mixed by sludge recirculation at 30 L/h (i.e. 36 turnover volumes per day) using a hose pump.

In this study, sewage sludge was co-digested with beverage waste to ensure adequate biogas for the FO experiment. After acclimatisation, the reactor was first operated using only the sewage sludge as the substrate (referred to as mono-AD) for 30 days. The organic loading rate during this period was 1.59 (kg COD/m^3.day). From day 31, the system was transitioned to the stage 1 of anaerobic co-digestion (denoted as AcoD-1), in which the digester was fed with a mixture of sewage sludge and beverage waste (95:5 %, v/v) to obtain an organic loading rate of 1.82 (kg COD/m^3.day) for 30 days. From day 61, ratio between sewage sludge and beverage waste was changed to 85:15% (v/v) to achieve approximately 50% increase in organic loading rate (2.30 kg COD/m^3.day) in the stage 2 of anaerobic co-digestion (denoted as AcoD-2).

2.2.3 Forward osmosis experimental protocol

All FO experiments were performed in four steps at room temperature. In the first step, the membrane pure water flux was determined for 1 hour using DI water as the FS and seawater as the DS. Then, sludge centrate was used as the FS, and the FO experiments were conducted

until 60% water recovery to evaluate carbon and nutrient enrichment. Throughout this second step, biogas was continuously sparged into sludge centrate. At specific time intervals, a 5 mL sample was collected from the FS for analyses. In the third step, hydraulic flushing of fouled membrane was conducted through replacing the feed and draw solutions by DI water and increasing the cross-flow velocity to 24 cm/s for 10 min. In the final step, pure water was determined again to evaluate flux recovery. DI water was used as the FS under the same experimental conditions as in the first step. In all FO experiments, initial volumes of feed and draw solutions were 1 and 3 L, respectively. The used high ratio of DS to FS volume aimed at minimizing the dilution effect of the DS during FO operation. The temperature, pH and conductivity of the FS were regularly monitored.

2.2.4. Membrane performance

Water flux (J_w) was calculated based on the change in weight of the DS, and expressed as in Eq.(1):

$$J_w = \frac{\Delta m_i}{\Delta t_i \times \rho \times A_m} \quad (1)$$

In which:

Δm_i: the change in weight of DS over a time interval (g); Δt_i: a time interval (hours); ρ: water density (g/cm^3); A_m: effective membrane area (m^2).

Water recovery was determined based on the ratio of the cumulative permeate volume and the initial volume of the FS, and presented as in Eq.(2):

$$\text{Water recovery } (\%) = \frac{\int_0^t J_w \times A_m \times dt}{V_{initial}} \times 100\% \quad (2)$$

In which:

J_w: the observed water flux at time t (LMH); $V_{initial}$: initial volume of the FS (L).

Solute rejection by the FO membrane was determined based on the mass balance, and presented as in Eq.(3):

$$\text{Rejection } (\%) = \left(1 - \frac{C_{DS_{(f)}} \times V_{DS_{(f)}} - C_{DS_{(i)}} \times V_{DS_{(i)}}}{C_{FS_{(i)}} \times V_{FS_{(i)}}}\right) \times 100\% \quad (3)$$

In which:

$C_{DS(i)}$ and $C_{DS(f)}$: the initial and final solute concentrations in the DS, respectively (mg/L); $V_{DS(i)}$ and $V_{DS(f)}$: the initial and final volumes of the DS, respectively (L); $C_{FS(i)}$: the initial solute concentration in the FS solution (mg/L); $V_{FS(i)}$: the initial volume of the FS (L).

2.3. Analytical methods

pH, electrical conductivity and temperature were measured using an Orion 4 – Star pH/conductivity meter (Thermo Scientific, Waltham, MA). COD was measured using a HACH DRB200 COD reactor and HACH DR3900 spectrophotometer following the US-EPA Standard Method 5220. Ammonia (NH_3-N) and total nitrogen (TN) were analysed using the US-EPA Standard Method 10205 and 10208, respectively and a HACH DR3900 spectrophotometer. Orthophosphate (PO_4^{3-}) was measured using ion chromatography (IC) (Thermo Fisher, Australia). The system was equipped with a Dionex AS-AP autosampler and a Dionex AS19 IC column (7.5 μm pore size, 4 mm diameter and 250 mm length). The sample injection volume was 10 μL. The sample was delivered in an isocratic mode with the hydroxide gradient (time [min]: concentration [mM]) (0-10: 10 10-25: 45; 25-27: 45; 27-30: 10; 31 stop run). The concentrations of Ca, Mg and other metal ions in sludge centrate were measured using an Inductively Coupled Plasma-Mass Spectrometry (Agilent 7900 ICP-MS).

The surface characteristics of the FO membranes were characterized using a scanning electron microscopy (SEM) and energy-disperse X-ray spectroscopy (EDS) system (i.e. a Zeiss Supra 55VP SEM and Oxford EDS system). A Bruker V70 Fourier transform infrared spectrometer was employed to test the Fourier transform infrared spectroscopy (FTIR) of fouled membrane samples and the wavenumber range was from 4000 to 600 cm^{-1}. Hydrophilicity of the membrane before and after fouled was characterized by measuring the contact angle using the sessile drop method at different locations. Zeta potential of the membrane was measured using the Malvern zeta analyser.

Biogas production was continuously recorded via the gas counter. Biogas composition was daily analysed using a portable GA5000 gas analyser (Geotechnical Instruments, UK) [23]. Alkalinity, total solid, and volatile solid were measured following the standard method 2320B and 5560C, respectively. Digestate pH was measured every second day following the aforementioned method.

3. Results and discussions

3.1. Biogas production

The increase in organic loading rate as a result of co-digestion led to an increase in daily biogas production without any discernible impacts on biogas composition (Figure 2). The high soluble and biodegradable COD content (Table 2) in beverage waste during co-digestion was favourable for biogas transformation. In details, the co-digestion with 45% increase in organic loading rate resulted in almost threefold increase in biogas yield (Figure 2). This observation could be explained by the synergistic effects reported in some previous studies [1, 23].

Negligible impacts of AcoD on biogas composition are evidenced by a slight increase in methane content compared to mono-AD with only sewage sludge (Figure 2). The increase in methane content appeared to be concurrent with minor improvements in COD and TS removal efficiency (Figure S2). These phenomena could be due to the highly biodegradable organic content in beverage waste as discussed above. These results were consistent with the observations from previous studies that have reported a slightly improved performance of AcoD system in terms of methane content, COD and TS removal [23, 24]. It is noted biogas composition was stable throughout all anaerobic digestion stage. The CO_2 content in biogas was about 35% (Figure S3).

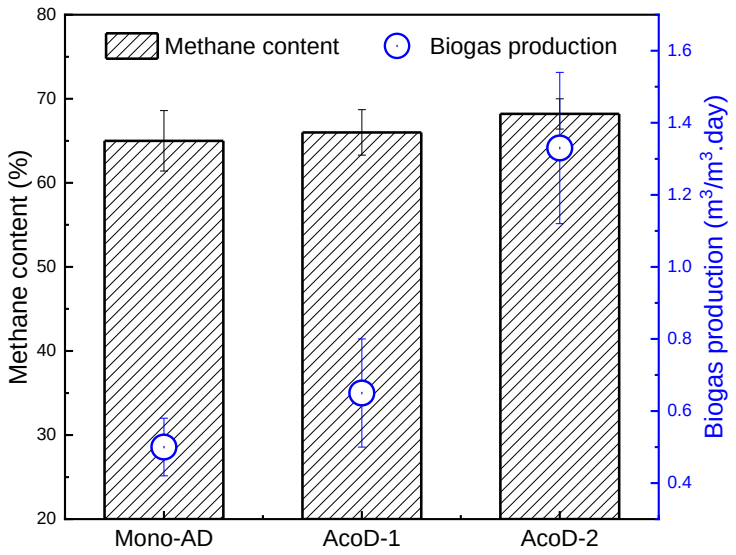

Figure 2. Performance of anaerobic co-digestion system in terms of biogas composition and production. Values and error bars are the mean and standard deviation of at least 20 samples.

3.2. The performance of seawater-driven FO system

3.2.1. Water flux and recovery

In all experiments, water flux decline was significant during the enrichment process. This flux decline was due mostly to the formation of cake layer (i.e. organic matter, inorganic substances and precipitates) on the membrane surface, and the dilution effect of DS caused by the water transportation from the FS to the DS. The results also indicated more severe fouling in PRO mode, compared to FO mode. This consequence resulted from the much higher pure water flux (i.e. 33 LMH), more severe concentration polarization (CP) and higher surface roughness of the supporting layer in PRO mode in comparison to FO mode [20]. Since less membrane fouling was observed in FO mode compared to PRO mode, FO mode was selected for biogas sparging experiments.

Compared to without biogas sparging, the system operated in FO mode with biogas sparging showed significant decrease in membrane fouling (Figure 3A). Without biogas sparging, water flux declined by over 95% towards both membrane orientations, while this value was only approximately 60% in FO mode with biogas sparging at water recovery of 60%. The decreased membrane fouling in FO mode with biogas sparging could be ascribed to the synergistic effects of smoothness of active layer in FO mode and changes in FS chemistry (i.e. pH and alkalinity). The impacts of FS chemistry modifications on fouling behaviour are discussed further in section 3.2.2. Less fouling in FO mode with biogas sparging could be supported by FTIR spectra of fouled membrane surface in different experimental conditions (Figure S4).

The highest flux recovery (92%) by physical flushing using DI water was observed in FO mode with biogas sparging (Figure 3B). The high flux reversibility in this case could be a result of less formation of compact cake layer on the membrane surface as discussed above. Moreover, once the fouled membrane surface was more hydrophilic in FO mode with biogas sparging, compared to the others (Figure S5), the affinity of fouling layer in this regard upon water was stronger. Thus, increased shear force produced by increasing cross-flow velocity could be capable of detaching the foulants from the membrane surface, thereby restoring water flux more efficiently.

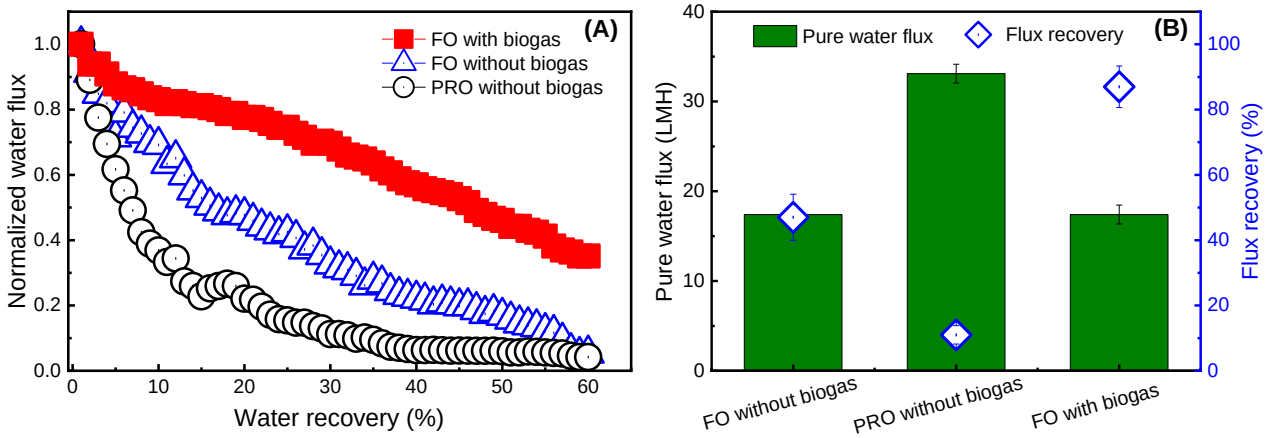

Figure 3. Effects of membrane orientation and biogas purging on (A) water flux and (B) fouling reversibility during seawater-driven FO pre-concentration of sludge centrate. Values and error bars are the mean and standard deviation of two replicate experiments.

Physical flushing was inefficient to remove fouling layer in FO and PRO modes without biogas sparging with less than 20% pure water flux recovery. This result is predominantly due to the enhanced aggregation and compaction of fouling layer caused by greater pure water flux [25], and the high roughness of supporting layer in PRO mode [26]. More compact fouling

297 layer is more challenging to be detached from the membrane surface. Greater roughness of
298 supporting layer led to weakening shear force created by physical flushing, thus reducing the
299 number of foulants swept away from the membrane surface.

300 **3.2.2. Improvement of organic carbon and nutrient enrichment**

301 Overall, FO pre-concentration of sludge centrate led to a proportional increase in organic
302 carbon content with water recovery, but FO mode with biogas sparging showed the best
303 enrichment performance (Figure 4A). In all cases, the experimental COD values were lower
304 than the maximum theoretical values that assumed complete COD retention by FO membrane.
305 Indeed, the COD rejection of the FO membrane is almost 100% (Figure S6). The observed
306 difference in COD enrichment between theoretical calculations and experimental results is
307 ascribed to the deposition of organic matter on the membrane surface. In fact, the efficiency of
308 COD enrichment was closely associated with the magnitude of fouling observed in section
309 3.2.1. The best performance of COD enrichment in FO mode with biogas sparging could be
310 attributed to the significant reduction in membrane fouling in this scenario. This result is well
311 supported by the observed magnitude of hydrophobicity of fouled membrane (i.e. PRO mode
312 with biogas > FO mode without biogas > FO mode with biogas) which may represent the level
313 of hydrophobic organic matter deposition on the membrane surface (Figure S5).

314 Without biogas sparging, the efficiency of nutrient enrichment during FO pre-concentration
315 of sludge centrate was decreased significantly (Figure 4B-D). This observation appeared to be
316 contrary to the expectation that the concentrations of nutrients are supposed to increase since
317 the FS is concentrated during the filtration according to mass balance and high nutrient
318 rejection by the FO membrane (Figure S6). The decrease in nutrient enrichment coincided with
319 increase in pH of the FS (Figure 5) and decrease in the amount of calcium ions in sludge
320 centrate (Figure 6). These observations suggest that low efficiency of nutrient enrichment can
321 be ascribed to the formation of precipitates (e.g. calcium phosphate ($Ca_3(PO_4)_2$), magnesium
322 phosphate ($Mg_3(PO_4)_2$) and struvite ($MgNH_4PO_4$)), and the conversion of ammonium ions to
323 ammonia gas at high pH. Indeed, the formation of these precipitates is likely to occur due to
324 the positive values of mineral saturation index (SI) [27] calculated for each precipitate (Table
325 S2). Calcium phosphate precipitation is likely to happen first with higher SI value (Table S2).
326 This statement is also consistent with the EDS analyses further discussed in section 3.3. In
327 addition to volatilisation, the significant decrease in ammonia enrichment is due to the low
328 rejection of the FO membrane upon the monovalent ion (i.e. NH_4^+ ions) (Table S5), and
329 electrostatic attraction between the negatively charged membrane surface (Table S1) and
330 ammonium ions.

By contrast, FO mode with biogas sparging demonstrated a remarkable improvement in nutrient enrichment (Figure 4B-D). With this technique, the enrichment of phosphate, ammonia and TN was almost similar to the theoretical enrichment curve. This observation is due to the inhibition of phosphorus precipitation, and the decreased conversion of ammonium ions to ammonia gas via volatilisation at decreased FS pH when using biogas buffering. Indeed, the pH of the FS decreased gradually and remained stable at around pH 7 during the filtration process (Figure 5). This pH value was not sufficiently favourable for the occurrence of phosphorous precipitation. In addition, the introduction of biogas into the system could increase the alkalinity of the FS via the dissolution of CO_2 into the aqueous solution. Carbonate ions can result in a competitive consumption of calcium ions, which hampers the formation of calcium phosphate precipitates [28]. This result is consistent with the changes in the nature of precipitates discussed further in section 3.3.

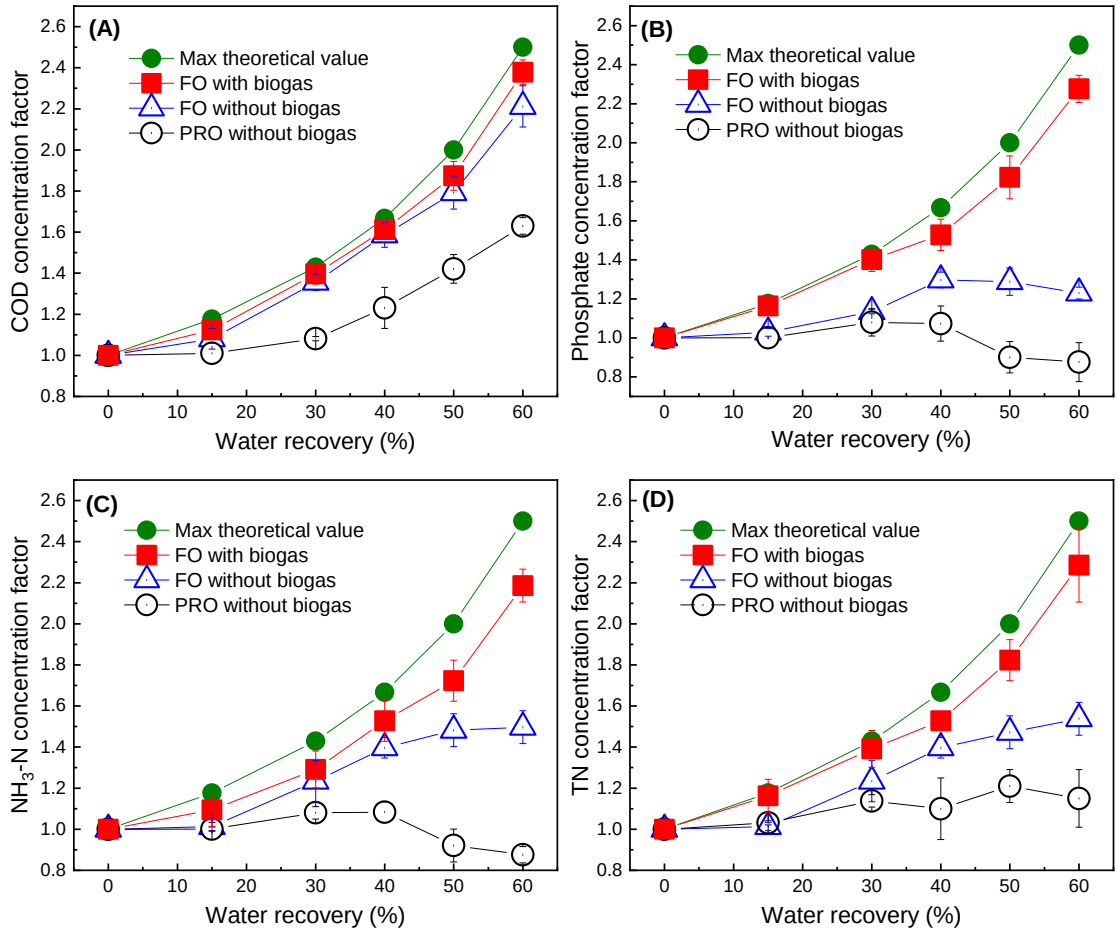

Figure 4. The enrichment of (A) bulk organic carbon, (B) phosphate, (C) ammonia and (D) TN during seawater-driven FO pre-concentration of sludge centrate with and without biogas sparging in different membrane orientations. The maximum theoretical value of each

constituent as a function of water recovery was calculated based on a mass balance assuming complete rejection by the membrane (actual rejection values are shown in the Supplementary Data). Values and error bars are the mean and standard deviation of two replicate experiments.

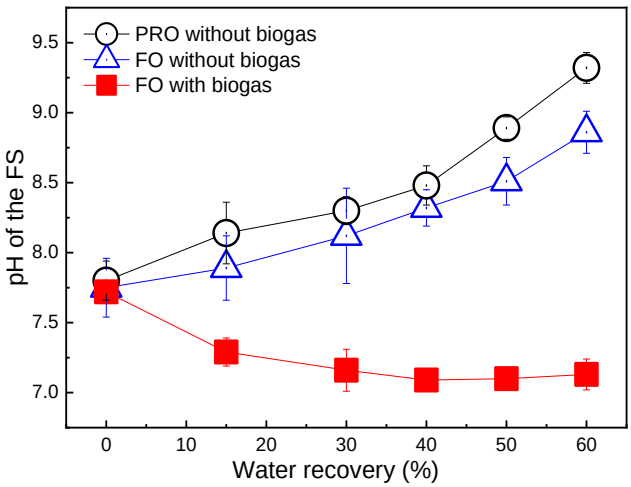

Figure 5. Variation in pH of the FS during seawater-driven FO pre-concentration of sludge centrate with and without biogas sparging in different membrane orientations. Values and error bars are the mean and standard deviation of two replicate experiments.

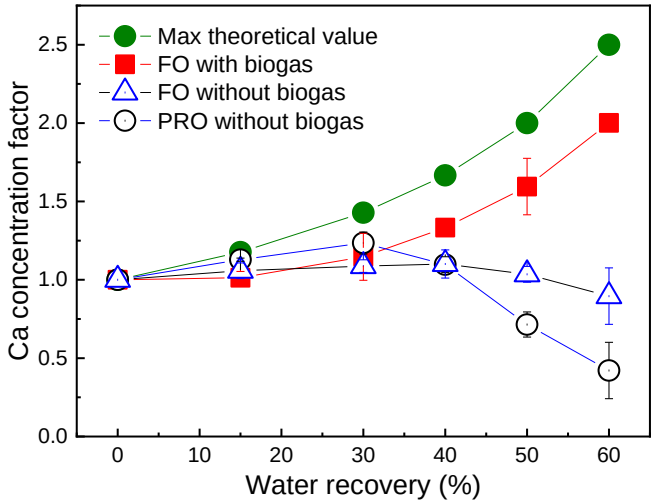

Figure 6. Variation in Ca concentration in the FS during seawater-driven FO pre-concentration of sludge centrate with and without biogas sparging in different membrane orientations. The maximum theoretical value of Ca as a function of water recovery was calculated based on a mass balance assuming complete rejection by the membrane (actual rejection values are shown in Table S1). Values and error bars are the mean and standard deviation of two replicate experiments.

The difference in nutrient enrichment behaviour between with and without biogas sparging could be elucidated through changes in pH of the FS, Ca concentration in the FS and filtration time during FO pre-concentration of sludge centrate (Figure 5 – 7). The increased FS pH (Figure 5) was concurrent with the decreased Ca concentration (Figure 6). This result indicated the formation of precipitates, which causes low nutrient enrichment without biogas sparging. The increase of the FS pH promoted precipitation that caused membrane fouling and more prolonged the filtration time (Figure 7). The results revealed that FO mode with biogas sparging demonstrated approximately eightfold decrease in filtration time, compared to PRO mode without biogas sparging at water recovery of 60% (Figure 7).

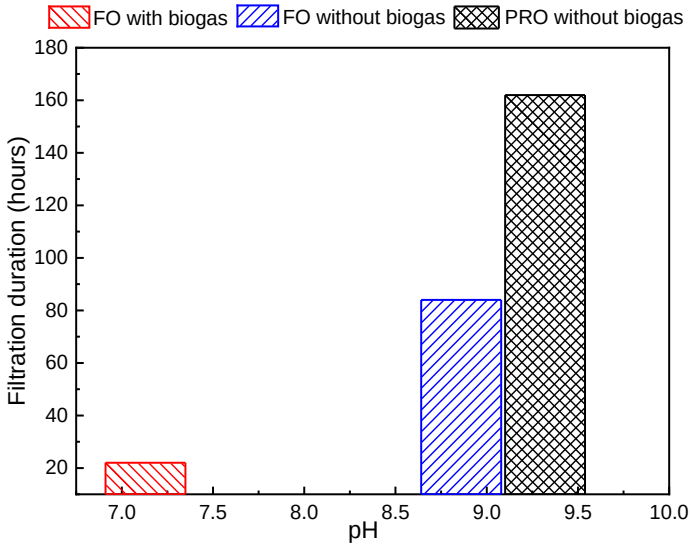

Figure 7. The correlation between FS pH and filtration duration towards different experimental conditions at water recovery of 60%.

3.3. Fouling characterization and fouling mitigation mechanisms

The microscopic analysis and elemental mapping of the fouling layer confirm the formation of Ca-P precipitates on the membrane surface during seawater-driven FO pre-concentration of sludge centrate (Figure 8A-D). The coarse membrane surface after enrichment process indicated the deposition of organic materials and precipitates on the membrane surface (Figure 8A and 8C). The fouling layer appeared to be more compact in PRO mode than in FO mode without biogas. This observation is consistent with the explanation discussed in section 3.2.1. The presences of Ca, P and O elemental peaks on the membrane surface indicated the composition of calcium phosphate precipitates. The observed stronger elemental peaks and denser distribution of Ca and P (Figure 8B and 8D) indicated more fouling in PRO mode, compared to FO mode without biogas sparging. In addition, the observed spherical particles on

the membrane surface are most likely to be amorphous calcium phosphates when compared to the literature [29].

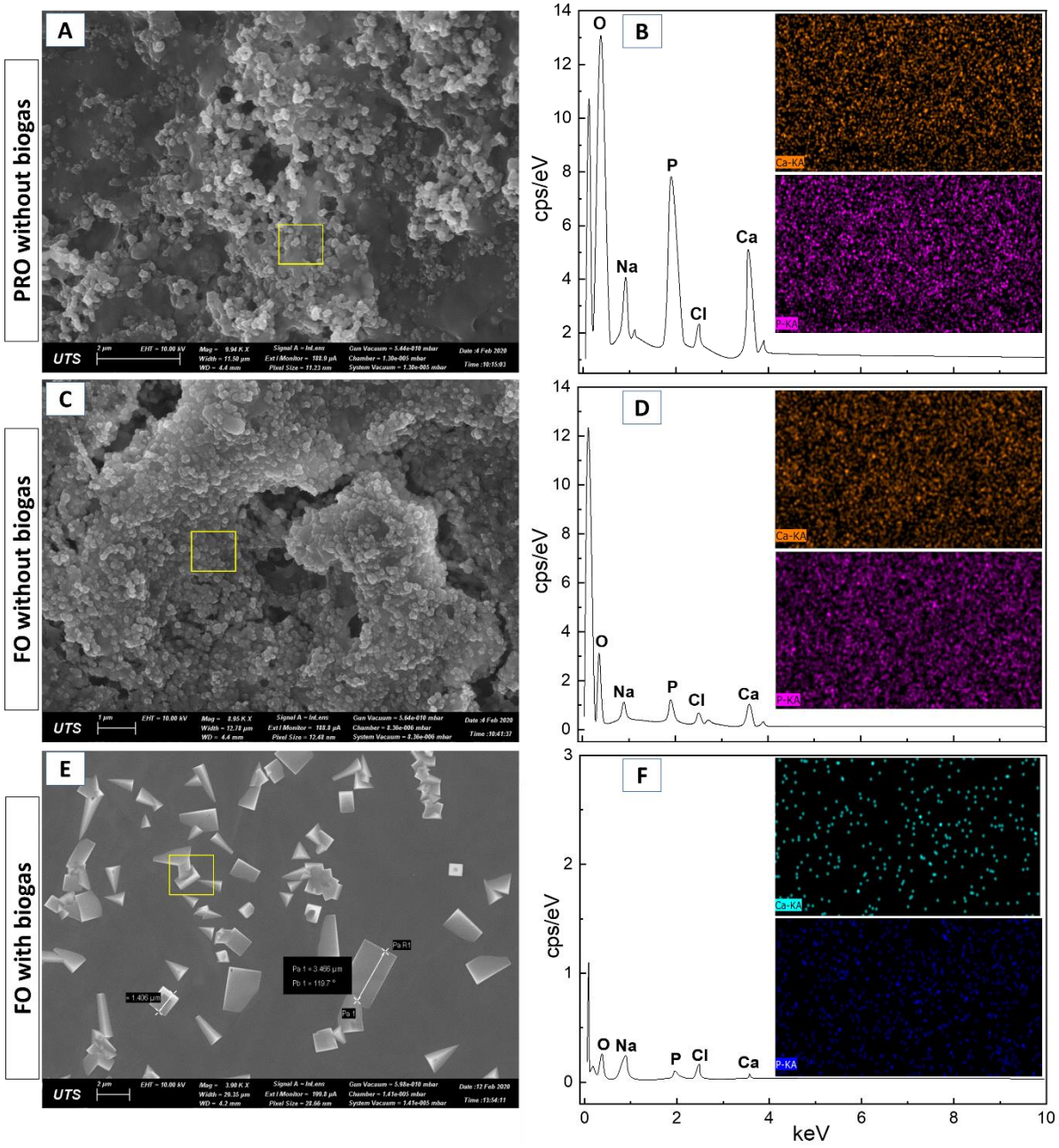

Figure 8. SEM and EDS mapping analyses of fouling layer on the membrane surface facing the FS towards without biogas sparging in PRO mode (A and B, respectively); without biogas sparging in FO mode (C and D, respectively) and with biogas sparging in FO mode (E and F, respectively). The EDS mapping was within the yellow squares.

The introduction of biogas into the FS resulted in the significant changes in morphology and elemental composition of fouling layer on the membrane surface (Figure 8E-F). Instead of a coarse fouling layer with sphere-like precipitates in the case of no biogas sparging, the membrane surface in FO mode with biogas sparging was covered by a smooth fouling layer

scattered with ikaite-like crystals. The formation of ikaite at low pH in the presence of phosphate were reported by Hu et al. (2015) [30]. The EDS elemental analysis (Figure 8F) revealed that biogas buffering significantly decreased the amounts of Ca, P and O content in the composition of the fouling layer. This result is strongly supported by the sparse distribution of Ca and P on the membrane surface via the mapping analysis (Figure 8F).

The above observations suggested possible mechanisms of using biogas buffering to mitigate fouling and improve the efficiency of seawater-driven FO enrichment of nutrients in sludge centrate. Biogas buffering controls the increase in the FS pH, thus minimizing the formation of phosphorous precipitates. This first mechanism is rigorously discussed in section 3.2 as well as strongly evidenced through the SEM and EDS mapping images shown above. In addition, the dissolution of CO_2 in biogas into the FS could increase its alkalinity, which may lead to the competitive reaction with phosphate. This mechanism is consistent with the results reported by Song et al. (2002) that the precipitation rate of phosphate was hindered significantly in the presence of carbonate at pH 8 or lower [31]. The formation of ion pairs between calcium and carbonate and the decrease of free calcium ions were shown to be the reasons for the decreased phosphate precipitation rate [31]. Indeed, the observation of ikite-like crystals in the fouling layer on the membrane surface in the conclusion of the filtration could confirm this mechanism.

4. Conclusion

This study demonstrated the feasibility of biogas sparging to control membrane fouling and improve the enrichment efficiency of a seawater-driven forward osmosis (FO) system that was used to pre-concentrate sludge centrate for subsequent nutrient and energy recovery. Biogas from anaerobic co-digestion of sewage sludge and beverage waste was used for this purpose. Without biogas sparging, severe membrane fouling and low organic and nutrient enrichment efficiency were observed. The observed low enrichment efficiency was due to the conversion of ammonium to ammonia, and the deposition of organic matter and Ca-P precipitates on the membrane surface at high feed solution pH during the enrichment process. By sparging biogas into sludge centrate, membrane fouling was significantly reduced, and the efficiency of organic matter and nutrient enrichment was close to theoretical values. In other words, organic and nutrient contents in sludge centrate increased proportionally against water recovery. FO membranes with biogas sparging demonstrated high fouling reversibility with almost 90% pure water flux recovery using only physical flushing. The enhanced nutrient enrichment and reduction in membrane fouling by sparging sludge centrate with biogas could be ascribed to the solubilisation of phosphate and ammonium at neutral pH due to carbonate buffering. Although biogas sparging is beneficial for subsequent resource recovery from sludge centrate,

potential issues associated with the odour and flammability of biogas (i.e. CH_4) should be rigorously taken into consideration. Indeed, the dissolved methane content in sludge centrate can reach up to 26 mg CH_4/m^3 [32]. The integrated technical and management solutions should be adopted to eliminate these problems. For example, aeration or degasification can be applied to remove methane gas from the concentrated sludge centrate after the filtration process [33]. Using a number of methods for venting CH_4, such as a vented tank, an air release valve, and air separator can be effective in mitigating the risk related to the dissolved methane. Also, the installation of intrinsically safe equipment for the membrane filtration and recovery systems can be crucial for the elimination of flammable and explosive risks derived from methane in sludge centrate.

5. Acknowledgement

The authors acknowledge financial support from the Australia Research Council, Australia through the ARC Research Hub for Energy-efficient Separation (IH170100009) for provision of financial support. Staff from the Cronulla Wastewater Treatment Plant are thanked for their assistance with the collection of raw sewage sludge, beverage waste and sludge centrate.

REFERENCES

[1] L. Mu, L. Zhang, K. Zhu, J. Ma, M. Ifran, A. Li, Anaerobic co-digestion of sewage sludge, food waste and yard waste: Synergistic enhancement on process stability and biogas production, Sci. Total Environ., 704 (2020) 135429.

[2] S. Xie, M.J. Higgins, H. Bustamante, B. Galway, L.D. Nghiem, Current status and perspectives on anaerobic co-digestion and associated downstream processes, Environmental Science: Water Research & Technology, 4 (2018) 1759-1770.

[3] Q. Wang, W. Zhang, Z. Yang, Q. Xu, P. Yang, D. Wang, Enhancement of anaerobic digestion sludge dewatering performance using in-situ crystallization in combination with cationic organic polymers flocculation, Water Res., 146 (2018) 19-29.

[4] R.W. Holloway, A.E. Childress, K.E. Dennett, T.Y. Cath, Forward osmosis for concentration of anaerobic digester centrate, Water Res., 41 (2007) 4005-4014.

[5] M.T. Vu, W.E. Price, T. He, X. Zhang, L.D. Nghiem, Seawater-driven forward osmosis for pre-concentrating nutrients in digested sludge centrate, J. Environ. Manage., 247 (2019) 135-139.

[6] H.P. Vu, L.N. Nguyen, J. Zdarta, T.T.V. Nga, L.D. Nghiem, Blue-green algae in surface water: Problems and Opportunities, Current Pollution Reports, 6 (2020) 105-122.

[7] J. Chen, S. Tang, F. Yan, Z. Zhang, Efficient recovery of phosphorus in sewage sludge through hydroxylapatite enhancement formation aided by calcium-based additives, Water Res., 171 (2020) 115450.

[8] T. Prot, W. Wijdeveld, L.E. Eshun, A.I. Dugulan, K. Goubitz, L. Korving, M.C.M. Van Loosdrecht, Full-scale increased iron dosage to stimulate the formation of vivianite and its recovery from digested sewage sludge, Water Res., 182 (2020) 115911.

[9] H. Wang, K. Xiao, J. Yang, Z. Yu, W. Yu, Q. Xu, Q. Wu, S. Liang, J. Hu, H. Hou, B. Liu, Phosphorus recovery from the liquid phase of anaerobic digestate using biochar derived from iron−rich sludge: A potential phosphorus fertilizer, Water Res., 174 (2020) 115629.

[10] A.J. Ansari, F.I. Hai, W.E. Price, J.E. Drewes, L.D. Nghiem, Forward osmosis as a platform for resource recovery from municipal wastewater - A critical assessment of the literature, J. Membr. Sci., 529 (2017) 195-206.

[11] Y. Li, Z. Xu, M. Xie, B. Zhang, G. Li, W. Luo, Resource recovery from digested manure centrate: Comparison between conventional and aquaporin thin-film composite forward osmosis membranes, J. Membr. Sci., 593 (2020) 117436.

[12] L. Zheng, W.E. Price, J. McDonald, S.J. Khan, T. Fujioka, L.D. Nghiem, New insights into the relationship between draw solution chemistry and trace organic rejection by forward osmosis, J. Membr. Sci., 587 (2019) 117184.

[13] A. Achilli, T.Y. Cath, A.E. Childress, Selection of inorganic-based draw solutions for forward osmosis applications, J. Membr. Sci., 364 (2010) 233-241.

[14] X. Bao, Q. Wu, W. Shi, W. Wang, Z. Zhu, Z. Zhang, R. Zhang, X. Zhang, B. Zhang, Y. Guo, F. Cui, Insights into simultaneous ammonia-selective and anti-fouling mechanism over forward osmosis membrane for resource recovery from domestic wastewater, J. Membr. Sci., 573 (2019) 135-144.

[15] T.N.-D. Cao, S.-S. Chen, H.-M. Chang, S.S. Ray, H.Q. Le, C.C. Duong, T.X. Bui, Evaluating the performance of polystyrene sulfonate coupling with non ionic Triton-X114 surfactant as draw solution in forward osmosis and membrane distillation systems, Environmental Technology & Innovation, 19 (2020) 100993.

[16] H.-M. Chang, S.-S. Chen, Y.-T. Chen, W.-S. Chang, C.-W. Li, N.C. Nguyen, S.S. Ray, D.T.N. Cao, Recovery of iodide as triiodide from thin-film transistor liquid crystal display wastewater by forward osmosis, J. Hazard. Mater., 403 (2021) 123637.

[17] S. Daly, A. Allen, V. Koutsos, A.J.C. Semião, Influence of organic fouling layer characteristics and osmotic backwashing conditions on cleaning efficiency of RO membranes, J. Membr. Sci., 616 (2020) 118604.

[18] C. Ding, M. Yi, B. Liu, C. Han, X. Yu, Y. Wang, Forward osmosis-extraction hybrid process for resource recovery from dye wastewater, J. Membr. Sci., 612 (2020) 118376.

[19] A.J. Ansari, F.I. Hai, W.E. Price, L.D. Nghiem, Phosphorus recovery from digested sludge centrate using seawater-driven forward osmosis, Separation and Purification Technology, 163 (2016) 1-7.

[20] M.T. Vu, A.J. Ansari, F.I. Hai, L.D. Nghiem, Performance of a seawater-driven forward osmosis process for pre-concentrating digested sludge centrate: organic enrichment and membrane fouling, Environmental Science: Water Research & Technology, 4 (2018) 1047-1056.

[21] M. Xie, L.D. Nghiem, W.E. Price, M. Elimelech, Toward resource recovery from wastewater: Extraction of phosphorus from digested sludge using a hybrid forward osmosis–membrane distillation process, Environmental Science & Technology Letters, 1 (2014) 191-195.

[22] T.Y. Cath, M. Elimelech, J.R. McCutcheon, R.L. McGinnis, A. Achilli, D. Anastasio, A.R. Brady, A.E. Childress, I.V. Farr, N.T. Hancock, J. Lampi, L.D. Nghiem, M. Xie, N.Y.

512 Yip, Standard methodology for evaluating membrane performance in osmotically driven
513 membrane processes, Desalination, 312 (2013) 31-38.

514 [23] R. Wickham, S. Xie, B. Galway, H. Bustamante, L.D. Nghiem, Anaerobic digestion of
515 soft drink beverage waste and sewage sludge, Bioresour. Technol., 262 (2018) 141-147.

516 [24] M.T. Vu, L.N. Nguyen, K. Li, Q. Fu, M.A.H. Johir, A. Fontana, L.D. Nghiem, Biomethane
517 production from anaerobic co-digestion and steel-making slag: A new waste-to-resource
518 pathway, Sci. Total Environ., (2020) 139764.

519 [25] Q. She, R. Wang, A.G. Fane, C.Y. Tang, Membrane fouling in osmotically driven
520 membrane processes: A review, J. Membr. Sci., 499 (2016) 201-233.

521 [26] M. Elimelech, Z. Xiaohua, A.E. Childress, H. Seungkwan, Role of membrane surface
522 morphology in colloidal fouling of cellulose acetate and composite aromatic polyamide reverse
523 osmosis membranes, J. Membr. Sci., 127 (1997) 101-109.

524 [27] S. Daneshgar, A. Buttafava, D. Capsoni, A. Callegari, G.A. Capodaglio, Impact of pH and
525 ionic molar ratios on phosphorous forms precipitation and recovery from different wastewater
526 sludges, Resources, 7 (2018).

527 [28] C. Barca, C. Gérente, D. Meyer, F. Chazarenc, Y. Andrès, Phosphate removal from
528 synthetic and real wastewater using steel slags produced in Europe, Water Res., 46 (2012)
529 2376-2384.

530 [29] M. Keskar, C. Sabatini, C. Cheng, M.T. Swihart, Synthesis and characterization of silver
531 nanoparticle-loaded amorphous calcium phosphate microspheres for dental applications,
532 Nanoscale Advances, 1 (2019) 627-635.

533 [30] Y.-B. Hu, M. Wolthers, D.A. Wolf-Gladrow, G. Nehrke, Effect of pH and phosphate on
534 calcium carbonate polymorphs precipitated at near-freezing temperature, Crystal Growth &
535 Design, 15 (2015) 1596-1601.

536 [31] Y. Song, H.H. Hahn, E. Hoffmann, The effect of carbonate on the precipitation of calcium
537 phosphate, Environ. Technol., 23 (2002) 207-215.

538 [32] X. Chen, J. Guo, G.-J. Xie, Y. Liu, Z. Yuan, B.-J. Ni, A new approach to simultaneous
539 ammonium and dissolved methane removal from anaerobic digestion liquor: A model-based
540 investigation of feasibility, Water Res., 85 (2015) 295-303.

541 [33] M.R.J. Daelman, E.M. van Voorthuizen, U.G.J.M. van Dongen, E.I.P. Volcke, M.C.M.
542 van Loosdrecht, Methane emission during municipal wastewater treatment, Water Res., 46
543 (2012) 3657-3670.

544